



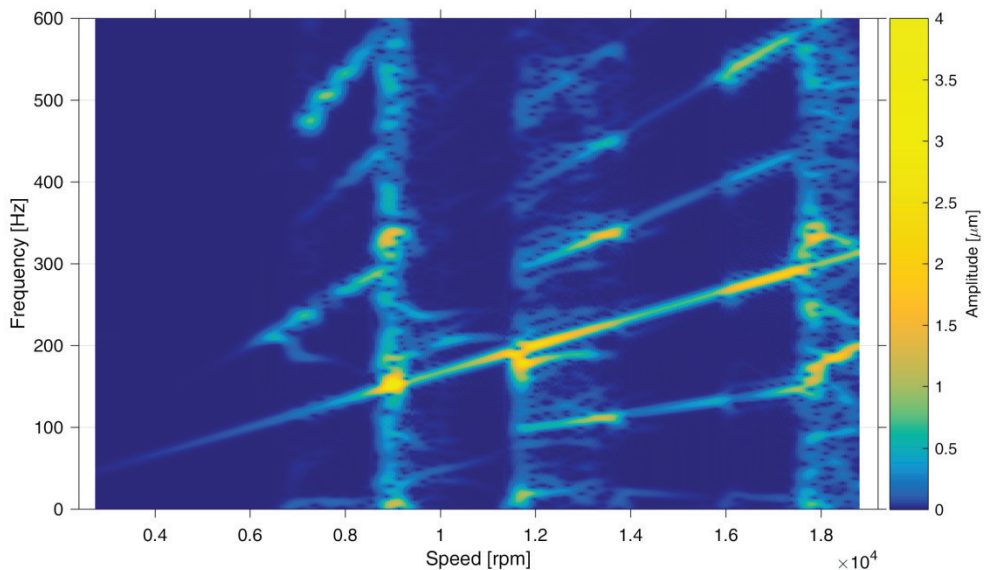
- 1 -

## Nonlinear Rolling Element Bearings in MADYN 2000 Version 4.3

In version 4.3 nonlinear rolling element bearings can be considered for transient analyses. The nonlinear forces are calculated with a module provided by [MESYS](#). Nonlinearities include clearance effects and the nonlinear Hertzian contact pressure. In the following effects caused by these nonlinearities are demonstrated for a typical rotor supported on deep groove ball bearings.

### Table of contents

1. Description of the System.....	2
2. Static Analysis, Gravitation Load and Axial Preload .....	3
3. Linear Analyses .....	5
3.1 Campbell Diagrams .....	6
3.2 Unbalance Response.....	8
4. Nonlinear Transient Analyses .....	11
4.1 Run Up with Axial Preload, Unbalance G2.5.....	12
4.2 Run Up without Axial Preload, Unbalance G2.5.....	15
4.3 Run Up without Axial Preload, Unbalance G1.0.....	19
5. Conclusions .....	23



Continue reading in case you want to learn how this spectrum arises.



- 2 -

## 1. Description of the System

The system can be seen in figure 1.1. The outer rings of the deep groove ball bearings are modelled as shafts. They are connected to the main shaft by “shaft in shaft connections” and the rolling element bearings, which are mounted between the shaft and the SBS connector. The outer shafts have only axial degrees of freedom. An axial preload is applied to the left bearing A for some studied cases (also see chapter 2). Bearing A is axially free, its outer ring is supported in axial direction by a weak axial spring. The outer ring of the right bearing B is rigidly supported in axial direction (stiffness infinite). It is an axially fixed bearing.

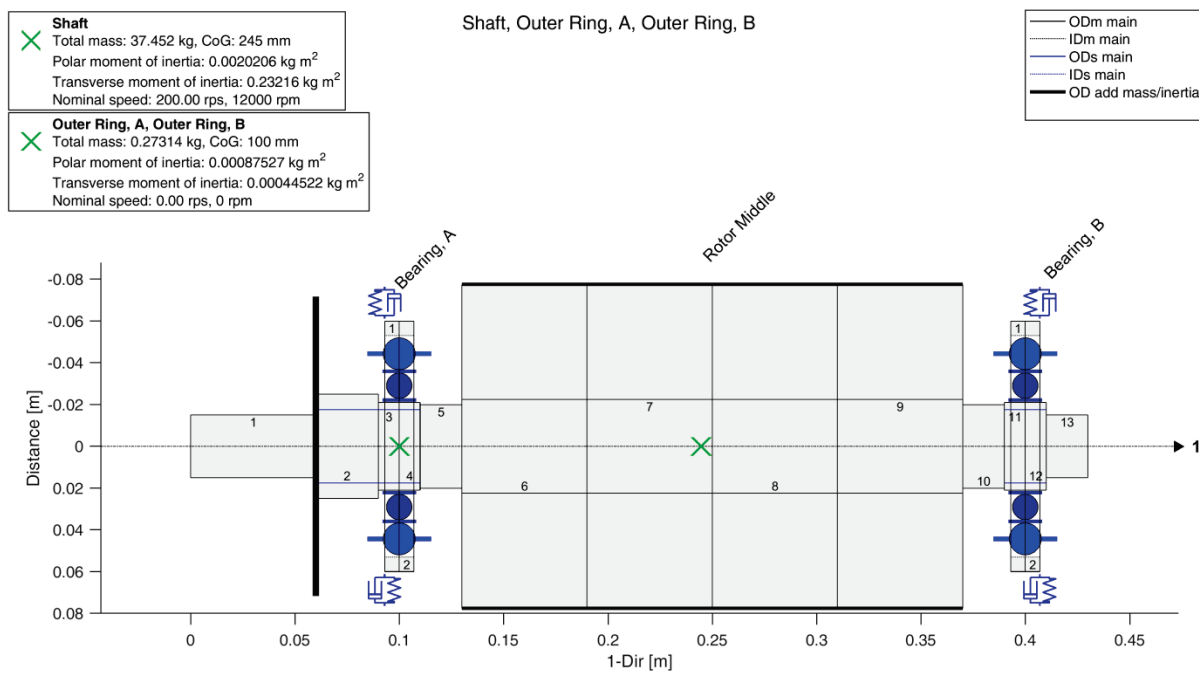


Fig. 1.1: System with deep groove ball bearings

The bearing has a diametric clearance of  $24\mu\text{m}$ .

The speed dependence of the bearings due to centrifugal and gyroscopic forces of the rolling elements is considered.



- 3 -

## 2. Static Analysis, Gravitation Load and Axial Preload

The rolling element bearings are loaded by the shaft weight and for some studied cases by the axial preloading, which is shown in figure 2.1.

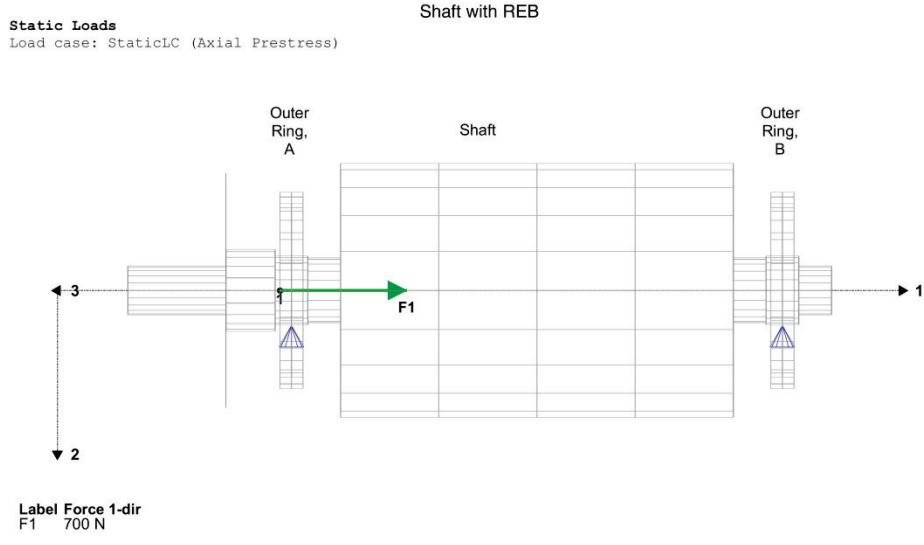


Fig. 2.1: Axial preload

The static forces for the load case weight and axial preload at 100% speed can be seen in figure 2.2. The displacements caused by the weight with and without axial preload at 100% speed are shown in figure 2.3 and 2.4. It is obvious, that the bearing without axial preload is much softer.

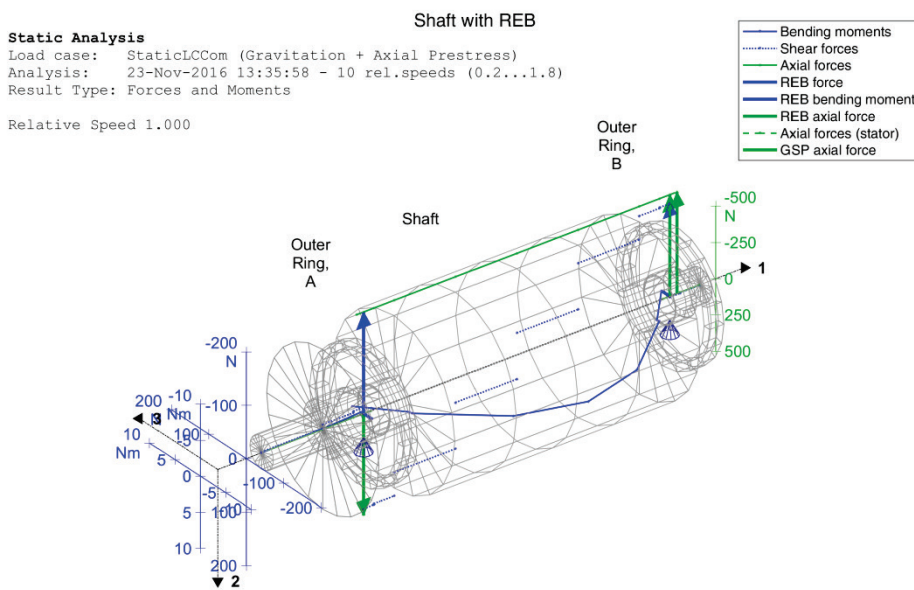
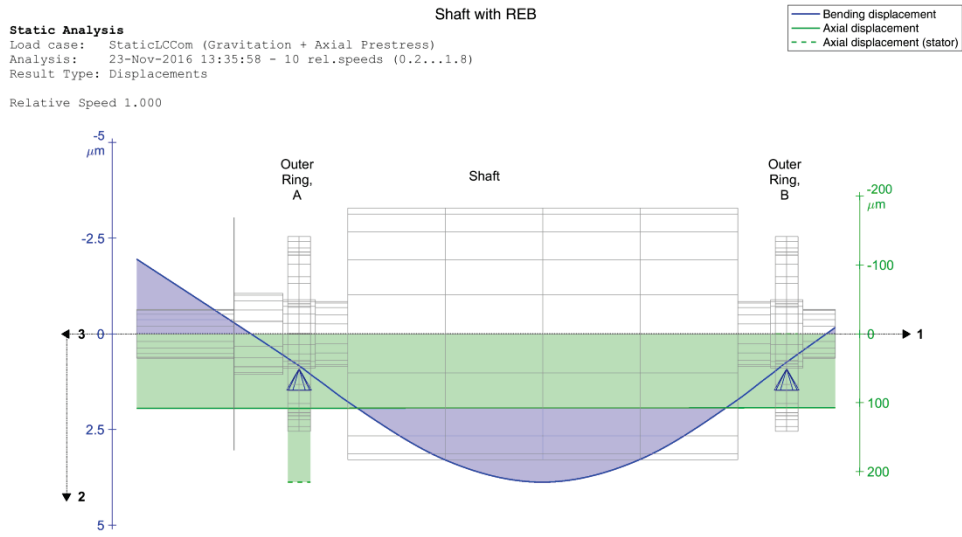


Fig. 2.2: Forces due to weight and axial preload at 100% speed

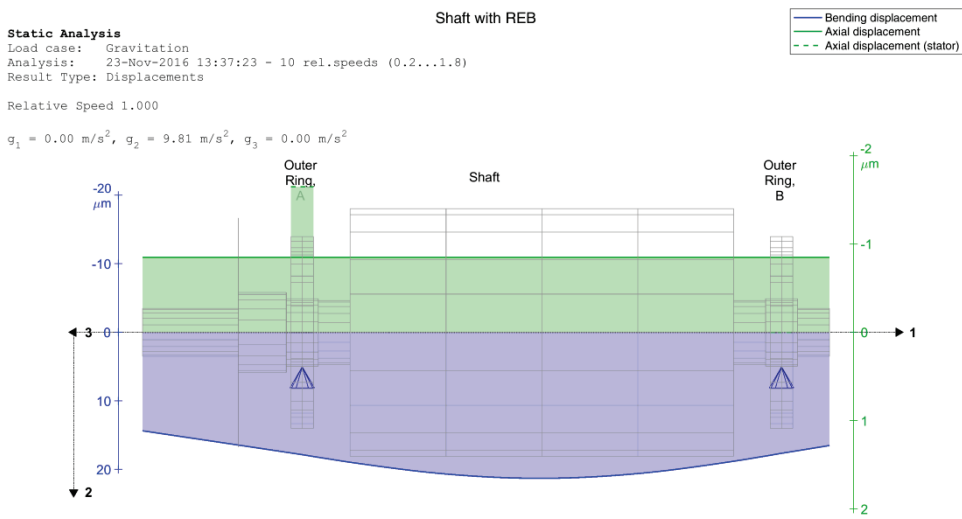


- 4 -



MADYN 2000 v.4.3.2

Fig. 2.3: Displacements caused by weight and axial preload



MADYN 2000 v.4.3.2

Fig. 2.3: Displacements caused by weight



- 5 -

### 3. Linear Analyses

The linear analyses are carried out with a linear 5x5 stiffness matrix including the coupling of radial lateral (2,3), bending rotational (5,6) and axial (1) coordinates, which can be seen in the following for bearing A with preload and without preload. The two matrices for bearing B are almost the same due to a similar loading.

Stiffness matrix with preload

Station 4, General Stiffness Matrix (inner/outer speeds 12000/0 rpm):						
	k1 [1/m]	k2 [1/m]	k3 [1/m]	k4 [1/rad]	k5 [1/rad]	k6 [1/rad]
[N]	5.4422e+07	-4.7763e+06	-0.0193	0	1.7045e-04	-60470.9280
[N]	-4.7838e+06	1.7525e+08	0.1052	0	-8.5059e-04	1.5457e+06
[N]	-0.0784	0.1052	1.7557e+08	0	-1.5484e+06	8.5071e-04
[N m]	0	0	0	0	0	0
[N m]	7.4027e-04	-9.6463e-04	-1.5678e+06	0	16003.5387	-7.7390e-06
[N m]	-61173.6994	1.5651e+06	9.6468e-04	0	-7.7368e-06	15988.0876

Stiffness matrix without preload

Station 4, General Stiffness Matrix (inner/outer speeds 12000/0 rpm):						
	k1 [1/m]	k2 [1/m]	k3 [1/m]	k4 [1/rad]	k5 [1/rad]	k6 [1/rad]
[N]	7.4059e+05	4032.5961	1.1573e-06	0	-1.1366e-08	-16632.3140
[N]	3966.3265	6.5667e+07	1.8190e-09	0	7.1054e-15	-4.7947
[N]	0	1.4934e-06	1.3648e+07	0	75.2693	0
[N m]	0	0	0	0	0	0
[N m]	-5.4606e-07	2.2985e-08	86.6294	0	54.4879	2.5201e-10
[N m]	-16764.5830	-58.3846	-2.2992e-08	0	2.5177e-10	379.2319

For the case with preload the stiffness in vertical 2-direction and horizontal 3-direction are almost equal (isotropic) and considerably higher than the anisotropic stiffness for the case without preload. The loaded 2-direction then is much stiffer than the unloaded 3-direction. Moreover the rotational stiffness about the 2- and 3-direction (coordinate 5,6) are much higher for the case with preload. Of course the same applies for the axial stiffness (direction 1).



- 6 -

### 3.1 Campbell Diagrams

The Campbell diagrams with natural frequencies up to 400Hz of the system with and without axial preload are shown in figure 3.1 and 3.2. The shapes with the bending component at 100% speed can be seen next to the diagram. For the system without preload the horizontal bending mode is below the nominal speed. The vertical bending mode is only slightly above nominal speed. The resonance of the axial mode for the preloaded system is close to 100% speed. For the system without preload it is much lower. This system has another axial mode, which is the mode of the left outer ring.

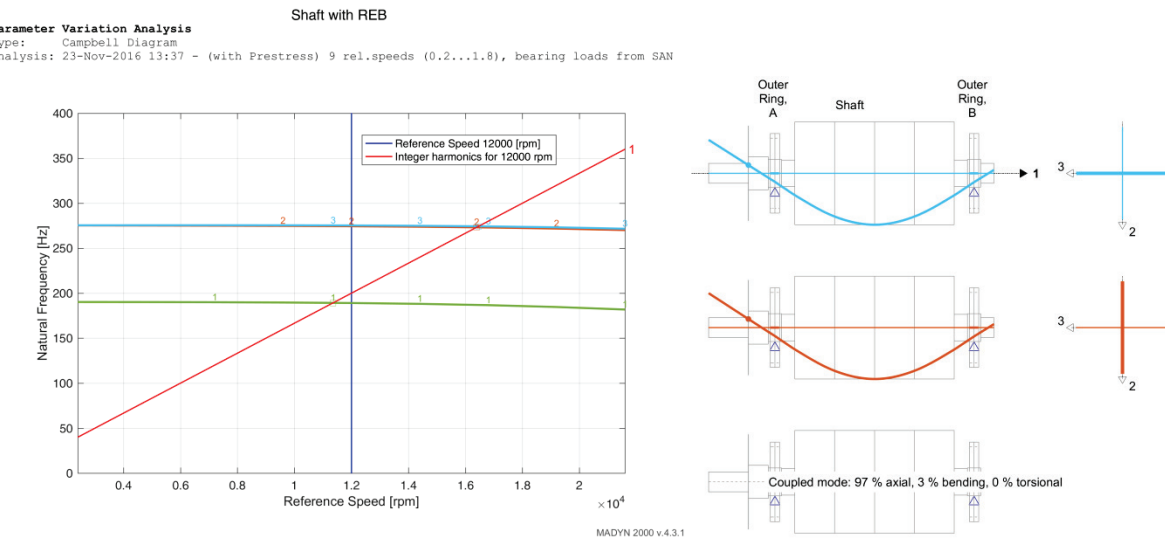


Fig. 3.1: Campbell diagram and mode shapes at 100% speed, system with axial preload

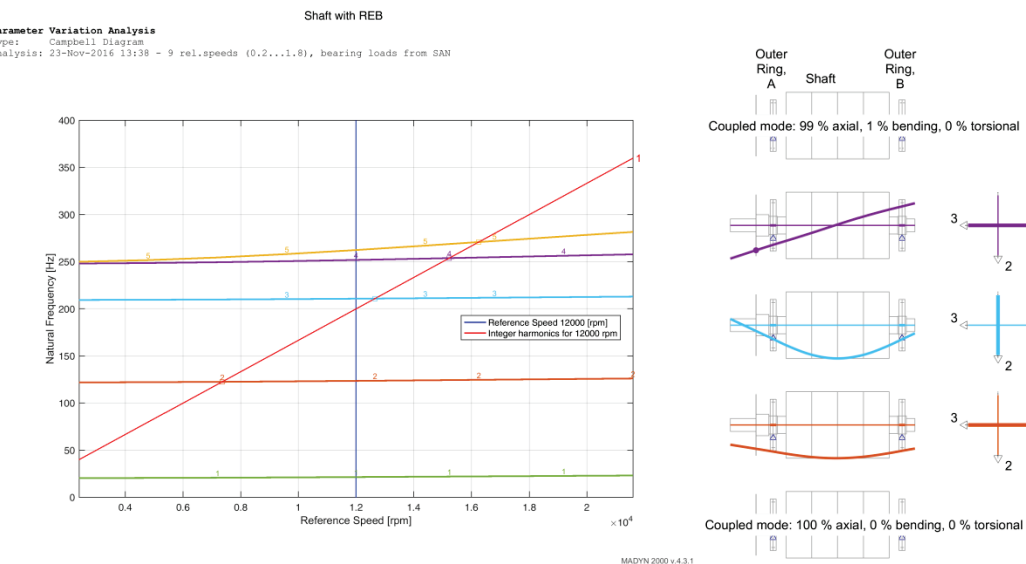


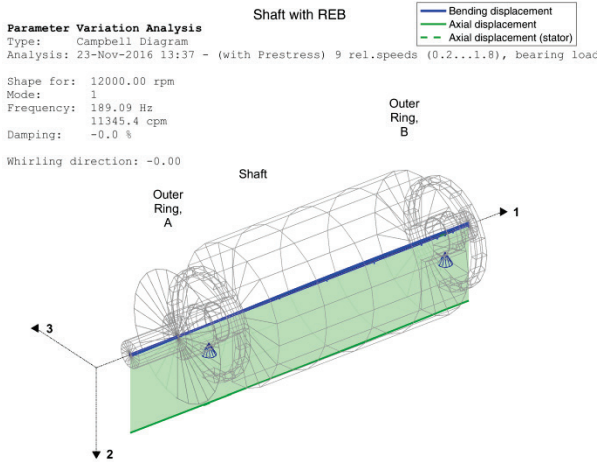
Fig. 3.2: Campbell diagram and mode shapes at 100% speed, system without axial preload

The coupled and non-bending mode shapes can be seen in figure 3.3 in 3D view with all components.

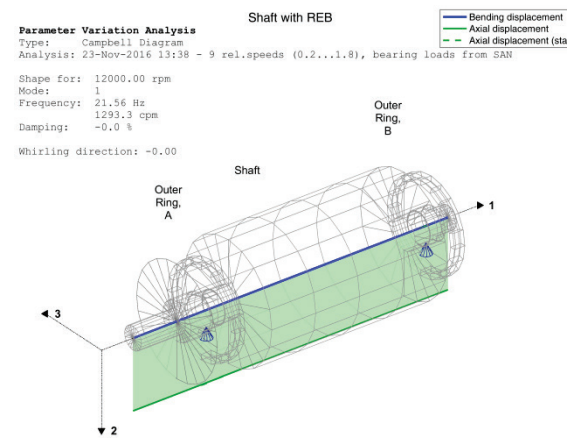


- 7 -

System with Preload



System without Preload



MADYN 2000 v.4.3.2

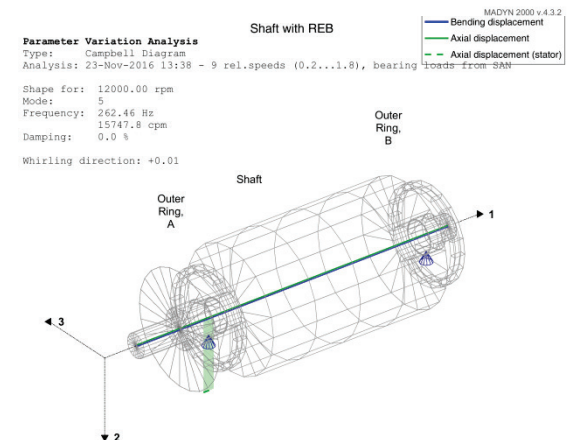
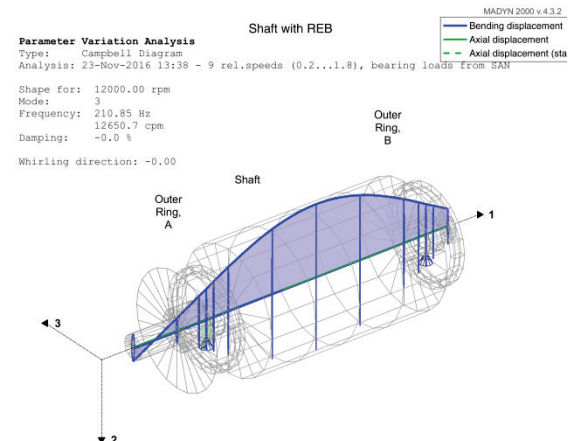


Fig. 3.3: Lateral axial coupled modes in 3D view with all components

MADYN 2000 v.4.3.2



- 8 -

### 3.2 Unbalance Response

The assumed unbalance load case is shown in figure 3.4. It corresponds to a balancing quality of G2.5.

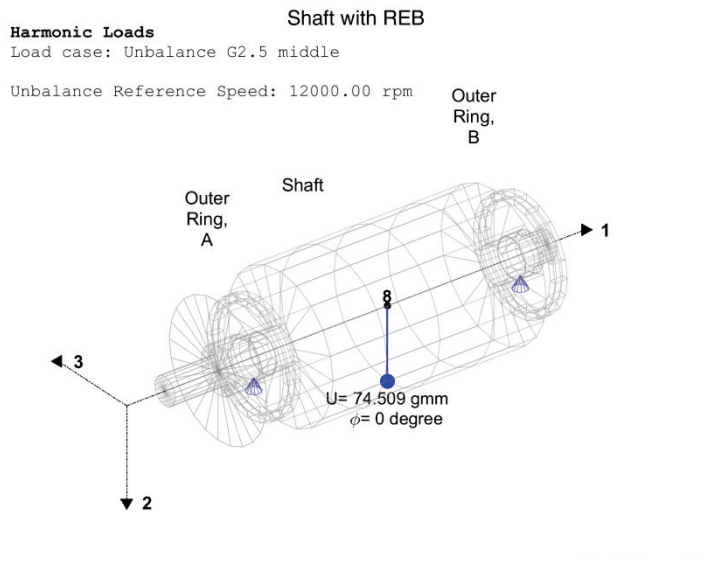


Fig. 3.4: Unbalance load case

All analyses for the harmonic response were calculated with a bearing damping proportional to the bearing stiffness. The proportionality factor yields a damping ratio of 1%, which is an input for rolling element bearings for harmonic response analyses.

In figures 3.5 to 3.8 the resonance curves of the radial displacements at the bearings and the radial bearing forces are shown for the two cases with and without axial preload.

The resonances can be clearly explained by the Campbell diagrams of the previous chapter. The lateral resonances are distinct and pronounced. The axial resonance with axially preloaded bearings at about 11'000 rpm is slightly visible in the radial response. For the axially unloaded case the axial mode at 15'500 rpm is visible as well in the radial response.

Later we will compare the linear and nonlinear vibration levels.



- 9 -

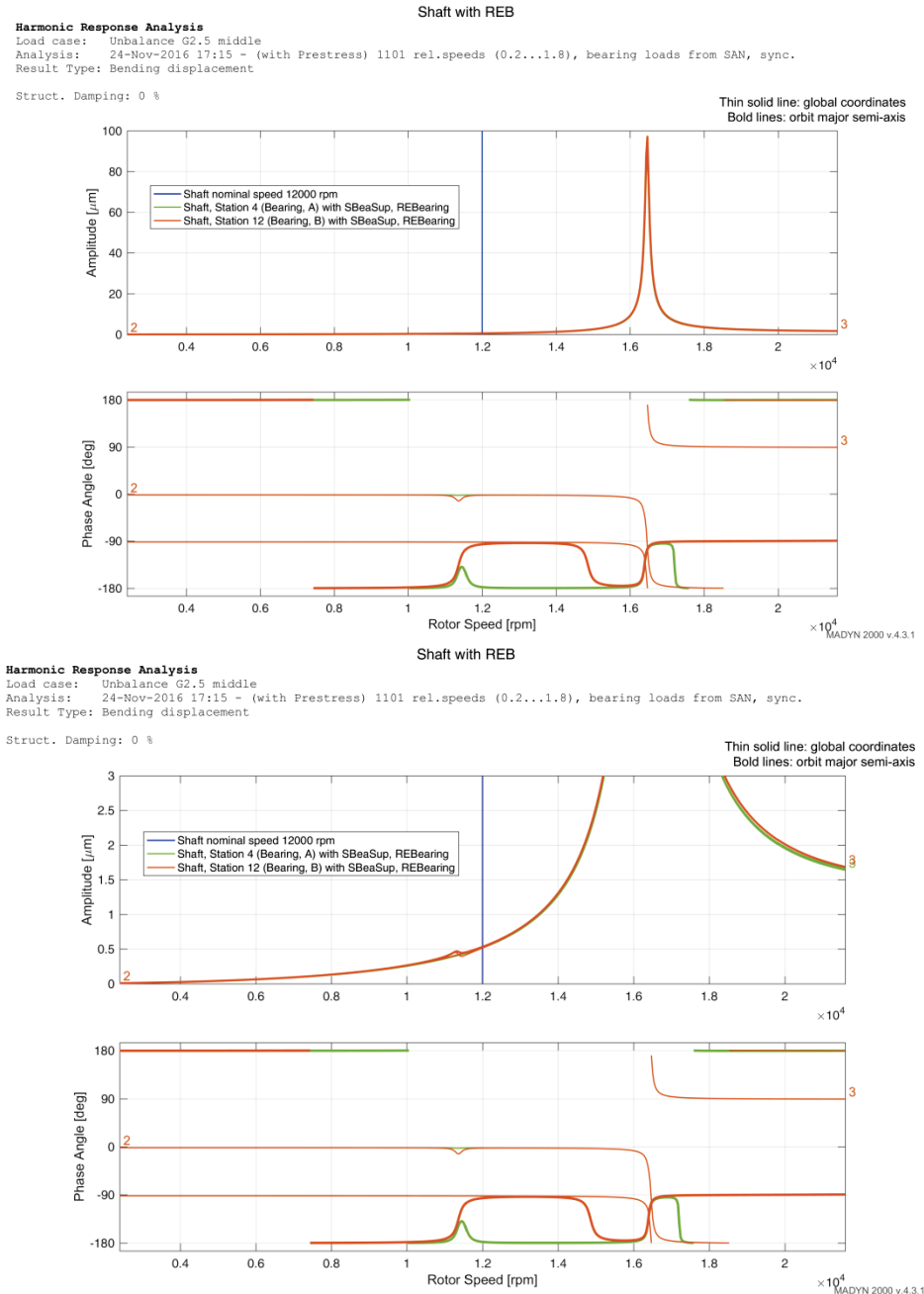


Fig. 3.5: Resonance curves of the radial displacements at the bearings with axial preload



- 10 -

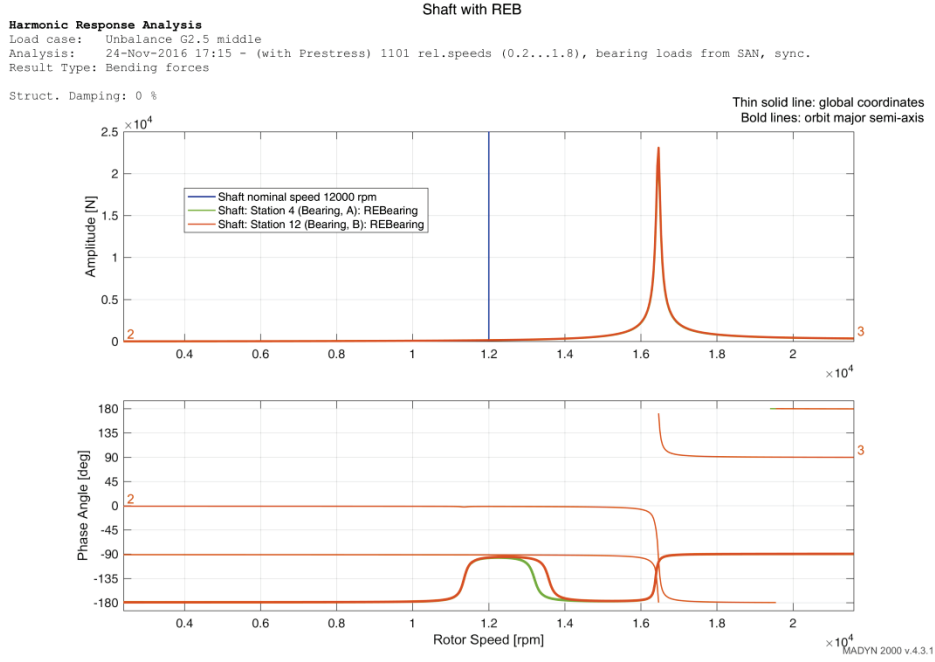


Fig. 3.6: Resonance curves of the radial bearing forces with axial preload

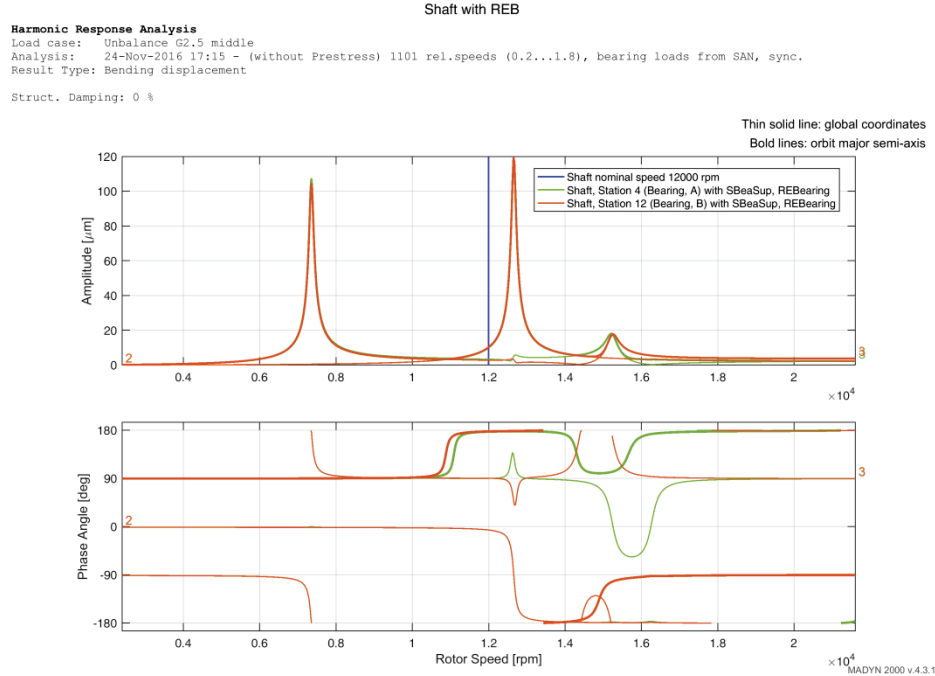


Fig. 3.7: Resonance curves of the radial displacements at the bearing without axial preload

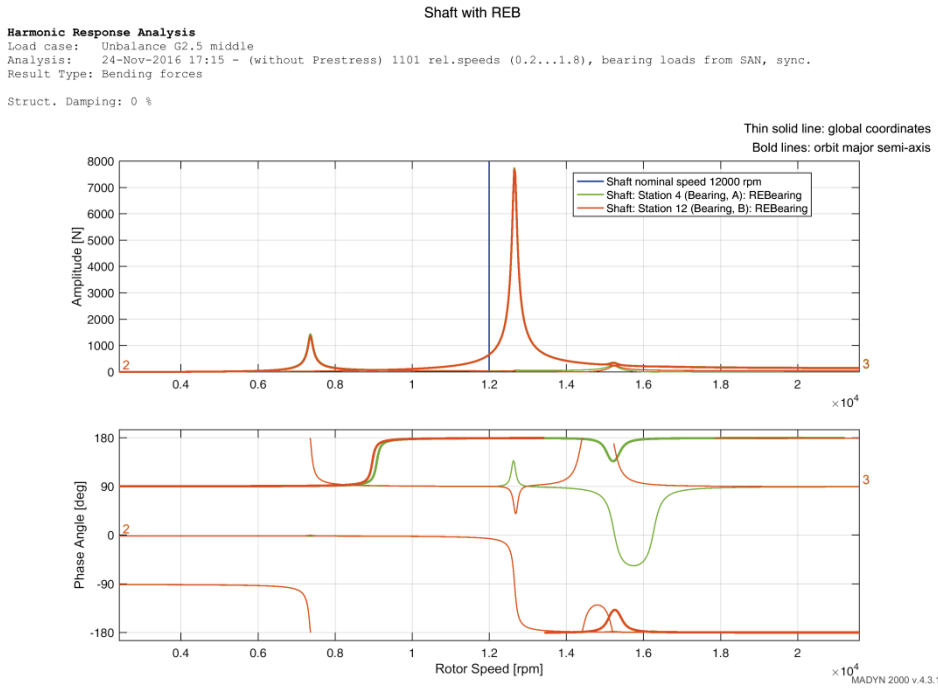


Fig. 3.8: Resonance curves of the radial bearing forces without axial preload

## 4. Nonlinear Transient Analyses

Nonlinear run up simulations from 20% to 160% nominal speed in 5s are carried out with the same unbalance load case as the linear analysis (see figure 3.4). Cases with and without axial preload are considered. For the case without axial preload an additional unbalance load case with lower unbalance level according to G1 is analysed in order to clearly demonstrate effects due to the nonlinear behaviour with clearance.

In all analyses a damping force proportional to the linear stiffness matrix is considered. The corresponding damping ratio for a frequency according to the current speed is 1%.

Results are shown as time history and orbit plots. In the time history plots the x-axes is rotor speed in rpm and not time in order to allow a better comparison with the linear resonance plots and a better interpretation by the Campbell diagram. Speed and time are directly linked by the speed versus time function  $n(t)$ ). Since the speed increase is linear, the plots versus speed are not distorted.



#### 4.1 Run Up with Axial Preload, Unbalance G2.5

The time histories of the radial displacements at the bearings for the run up are shown in figure 4.1. The corresponding orbits can be seen in figure 4.2. The time histories of the axial displacements at the bearings are shown in figure 4.3 and the radial bearing forces in figure 4.4.

The maximum vibration occurs at about 15'500rpm, which is at a lower speed than in the linear analysis. Below this speed the displacements agree well with the linear analysis (see for example the displacements at 12'000rpm in figure 3.5 and figure 4.1, enlarged plots). In the nonlinear analysis the increase of the vibration when approaching the resonance is much steeper, but the vibration starts decaying at a speed lower than the linear resonance. It seems the stiffness of the bearing in the nonlinear case is lower, which can be explained by the axial displacement in figure 4.3. Due to the high radial loading of the bearing when approaching the resonance, the balls of the bearing seek a more centred position in the groove, which results in an axial shift of the shaft. The new contact angle seems to yield a lower stiffness in spite of the high radial load.

In order to check this, the stiffness matrix with the loading at 15'500rpm can be calculated with MESYS. The resulting matrix can then be compared to the stiffness matrix of the linear analysis (see beginning of chapter 3).

Loading at 15'500rpm (radial force, axial force, rotational displacement):

Radial force in 2-direction: 2'388 N

Axial force: 700 N

Rotational displacement about 3 axis: -0.4021 mrad

The resulting stiffness matrix can be seen in the following with the relevant coefficients highlighted:

	k1 [1/m]	k2 [1/m]	k3 [1/m]	k4 [1/rad]	k5 [1/rad]	k6 [1/rad]
[N]	2.3042e+07	4.3191e+07	0	0	0	-4.4415e+05
[N]	4.3169e+07	<b>1.5407e+08</b>	0	0	0	-8.6310e+05
[N]	0	0	9.0014e+07	0	5.0731e+05	0
[N m]	0	0	0	0	0	0
[N m]	0	0	5.1300e+05	0	4391	0
[N m]	-4.4460e+05	-8.7200e+05	0	0	0	<b>9162</b>

Indeed the radial stiffness in the loaded direction 2 and the rotational stiffness about the 3-axis (coordinate 6) are lower. Using these stiffness values for an isotropic support yields a critical speed of 15'000rpm.

The effect of a lower resonance frequency compared to the linear analysis is smaller for a lower unbalance as additional analyses have shown.

Above the resonance the radial displacements of the linear and nonlinear analyses agree well.

The maximum vibration is lower than in the linear analysis (about one fourth). To some extent this is due to the unsteady condition during transient run up.

The maximum bearing forces for the nonlinear transient analysis are much lower (almost one tenth).



- 13 -

### Shaft with REB

#### Transient Response Analysis

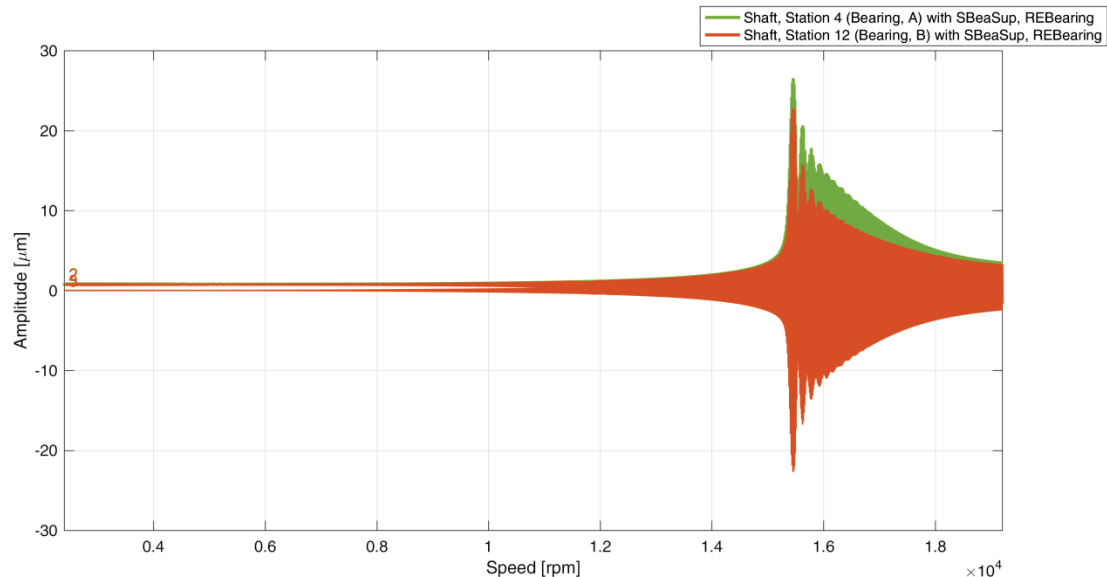
Load case: TransientNTCom 1 (Weight, Prestress, Unbalance G2.5)

Analysis: 23-Nov-2016 14:14:59 - n(t), (with Prestress G2.5) , init.cond. from SAN, nonlinear

Result Type: Bending displacement

Add. Modal Damping (all modes): 1 %

Bold lines correspond to directions 2 and 2'



MADYN 2000 v.4.3.1

### Shaft with REB

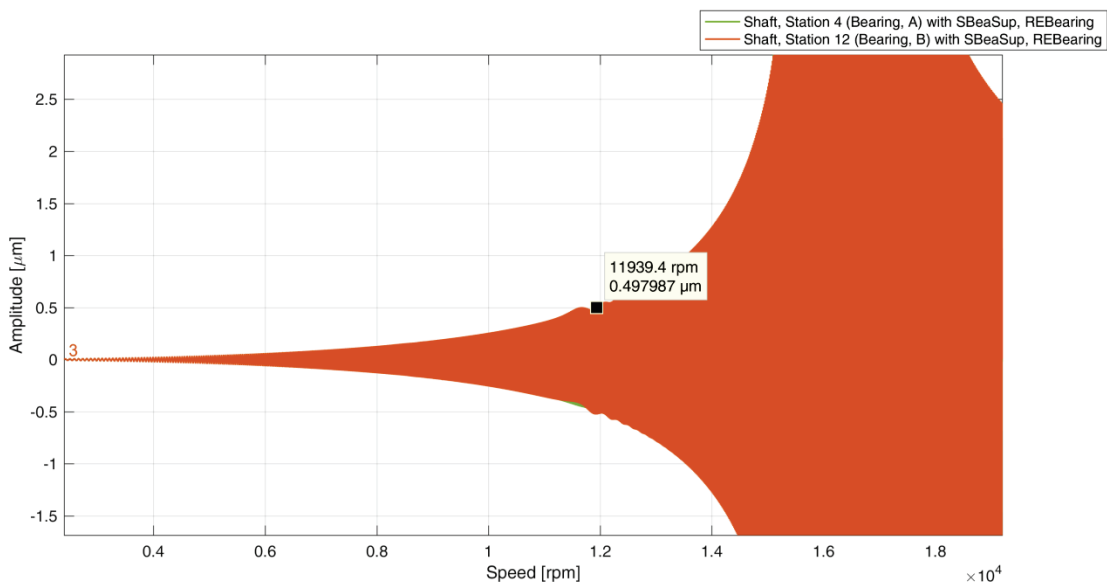
#### Transient Response Analysis

Load case: TransientNTCom 1 (Weight, Prestress, Unbalance G2.5)

Analysis: 23-Nov-2016 14:14:59 - n(t), (with Prestress G2.5) , init.cond. from SAN, nonlinear

Result Type: Bending displacement

Add. Modal Damping (all modes): 1 %



MADYN 2000 v.4.3.1

Fig. 4.1: Radial displacements at the bearings, run up from 20% to 160% in 5s, with axial preload



- 14 -

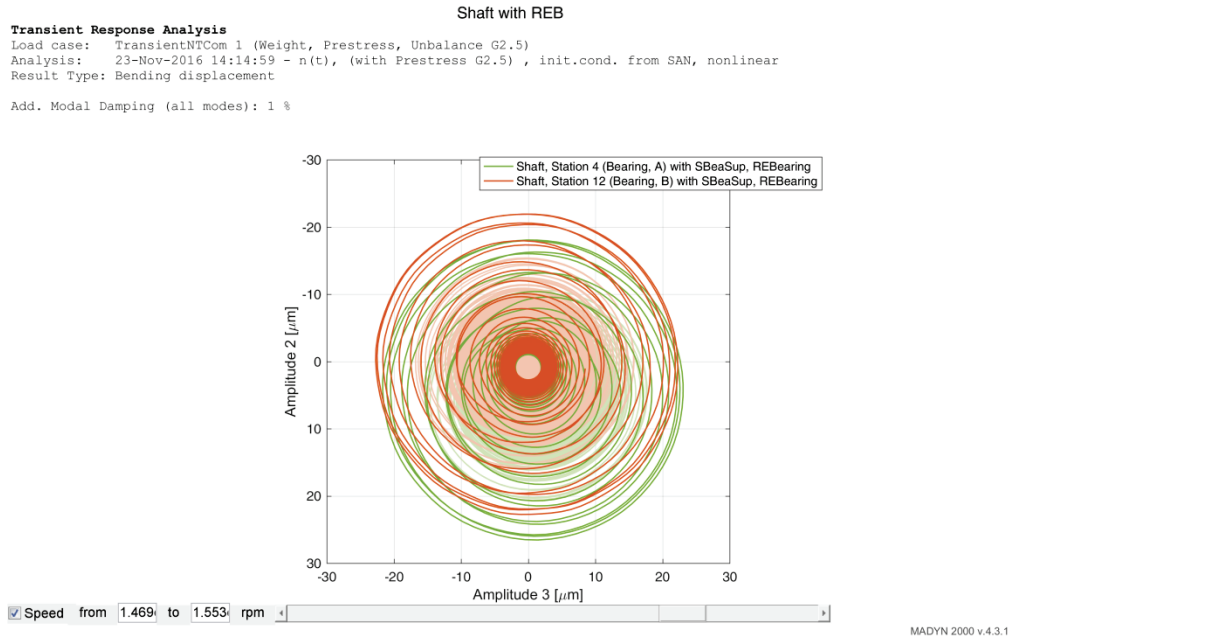


Fig. 4.2: Orbit plots at the bearings during run up with axial preload, speed range 14'700rpm to 15'530rpm highlighted

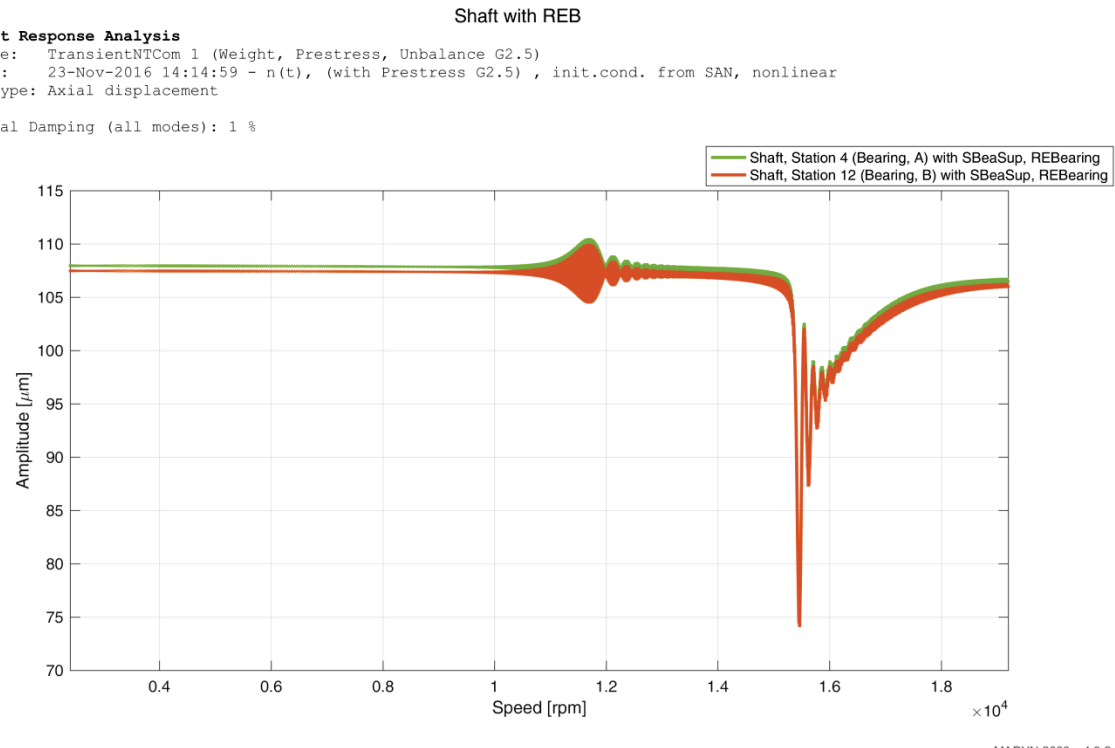


Fig. 4.3: Axial displacements at the bearings, run up from 20% to 160% in 5s, with axial preload



- 15 -

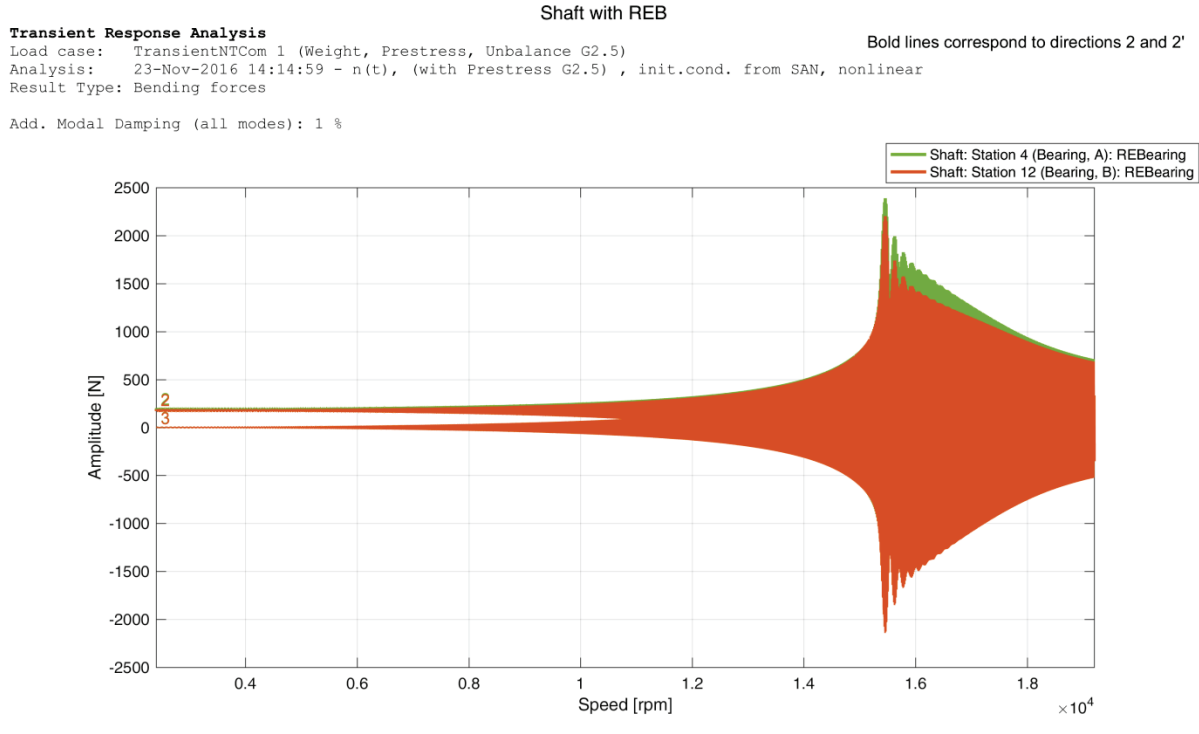


Fig. 4.4: Radial bearing forces, run up from 20% to 160% in 5s, with axial preload

## 4.2 Run Up without Axial Preload, Unbalance G2.5

The time histories of the radial displacements at the bearings for the run up of this case are shown in figure 4.5. A spectrum of the vibration of bearing A in 3-direction is shown in figure 4.6. The orbits at selected speeds at the bearings can be seen in figure 4.7. The time histories of the axial displacements at the bearings are shown in figure 4.8 and the radial bearing forces in figure 4.9.

In contrast to the linear analysis, where clear resonances in horizontal and vertical direction occur, only one clear resonance occurs in case of the nonlinear analysis. The speed is approximately the same as for the case with axial preload (app. 15'250rpm, see figure 4.5). Again an axial shift of the rotor can be observed as the rotor approaches the resonance, although there is no axial displacement outside the resonance and the balls should already be centred in the groove. The axial shift here is caused by the bending of the shaft, when approaching the resonance. The bending of the shaft would change the contact angle and an axial load would arise. Since an axial load cannot arise due to the axially loose bearing an axial shift occurs.

The spectrum in figure 4.6 and the orbits in figure 4.7 reveal nonlinear behaviour outside the maximum vibration due to the bearing clearance. At 8'000rpm the rotor does not fully whirl within the bearing clearance. The unbalance force is too weak to lift the rotor to an upper contact. At this speed the unbalance is an excitation to a rocking motion of the shaft. Such motion typically has a frequency component of half the excitation frequency, i.e. half the speed as they are visible in the spectrum at about 6'500rpm and 8'500rpm. Between these speeds the 1xn synchronous component suppresses the sub-synchronous, because there is a resonance at approximately 7'400rpm (see linear results in figure 3.2 and 3.7). At 10'000rpm the shaft fully whirls with a circular orbit. The vibration level is higher than in the linear analyses due to additional component of the clearance and the higher loading of the bearing caused by this additional component.



- 16 -

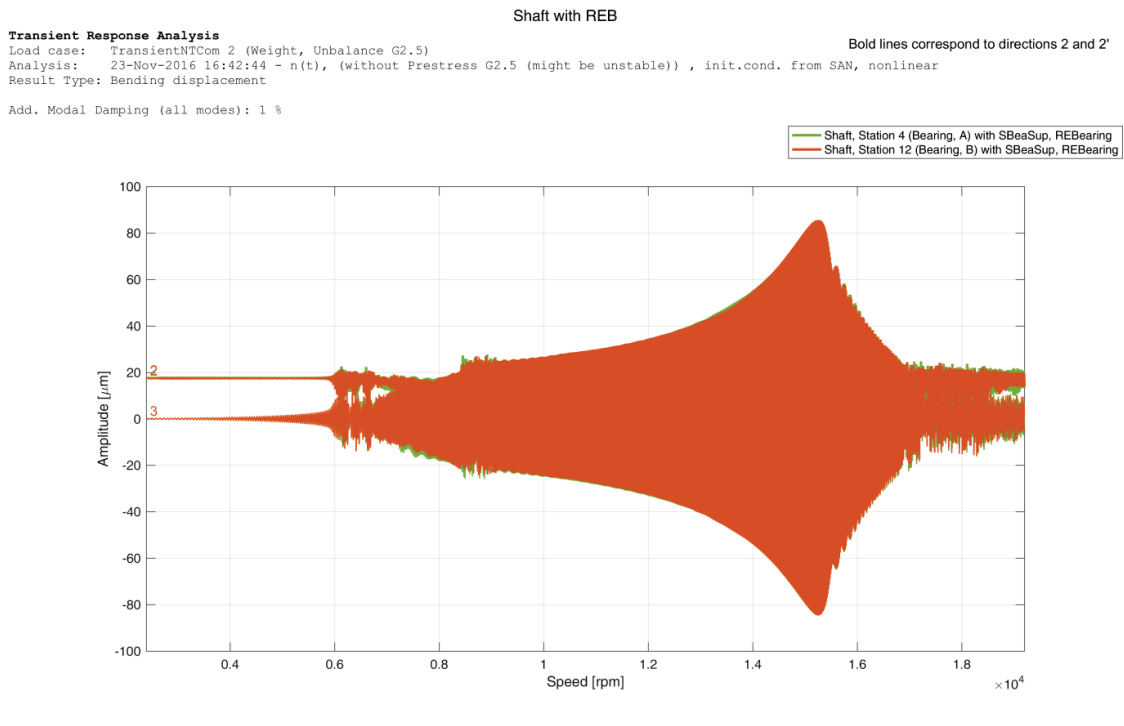


Fig. 4.5: Displacements at the bearings, run up from 20% to 160% in 5s, without axial preload

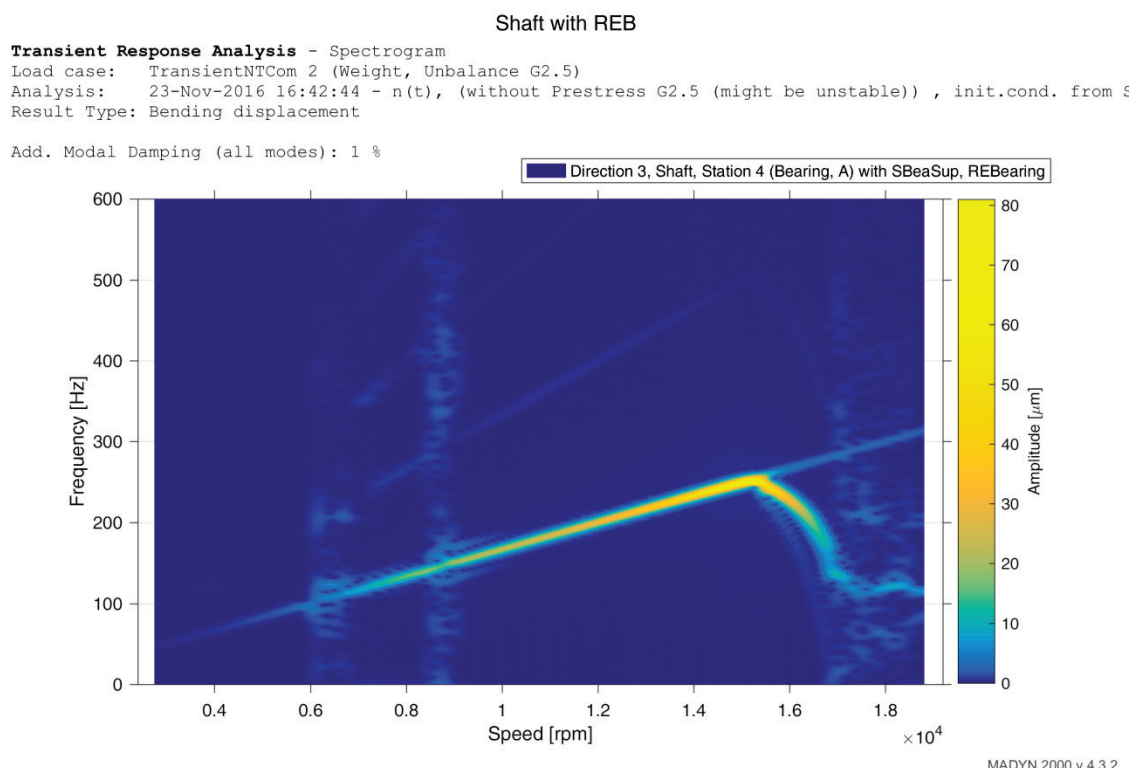


Fig. 4.6: Spectrum of the displacements at bearing A in 3-direction

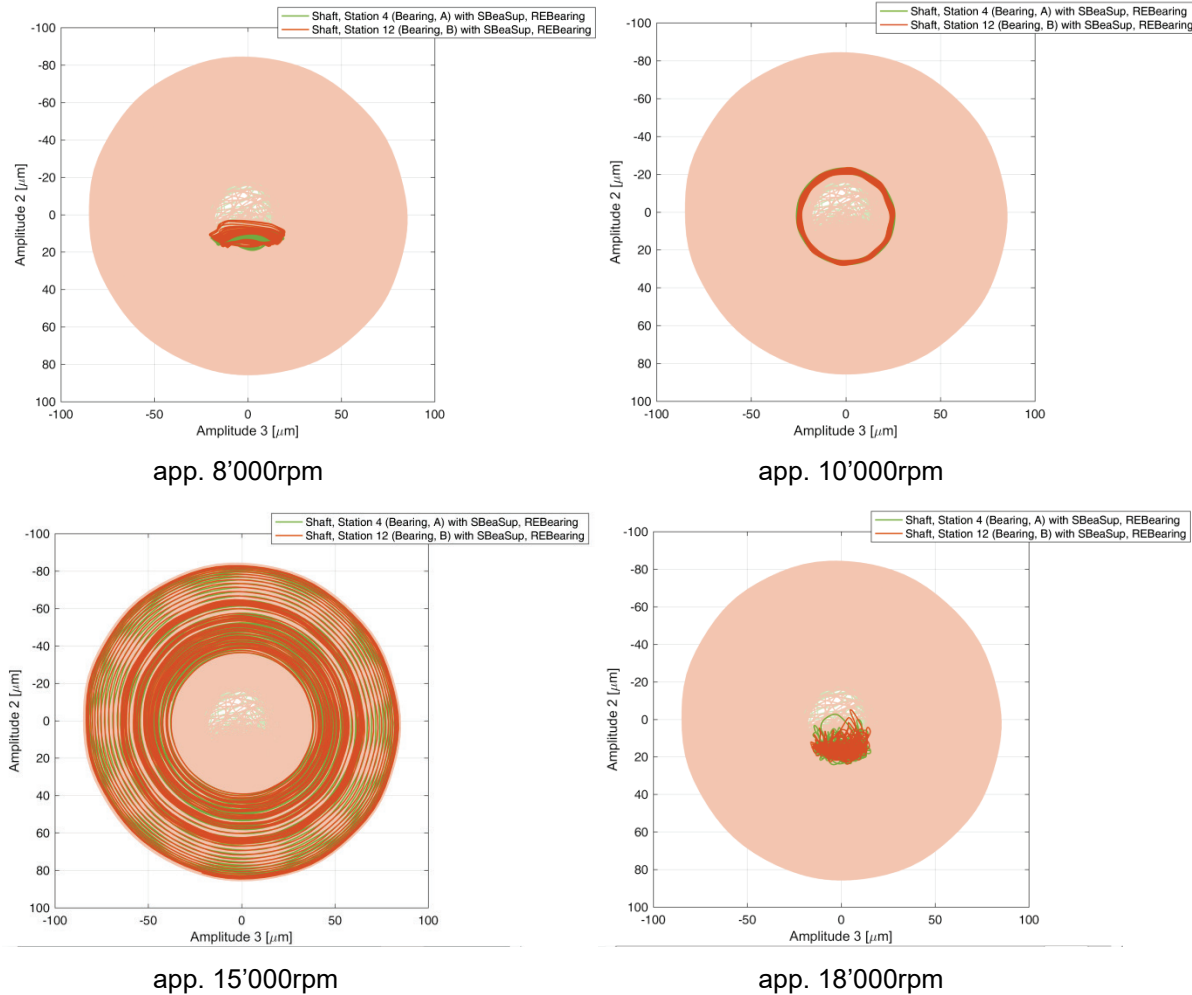


Fig. 4.7: Orbits at the bearings during run up, without axial preload

At speeds above resonance, the shaft again does not fully whirl (see orbit in figure 4.7 at 18'000rpm), because the response from the unbalance is small due to the self-centring effect. The vibration of the shaft then again is a kind of rocking motion and a strong component with a frequency close to half the speed appears (see spectrum in figure 4.6).

The vibration increase from speeds at about 8'000rpm to the maximum vibration at 15'250rpm is moderate resulting in a maximum, which is below the level of the resonance peak of the linear analysis in vertical direction (app. 30% lower).

The maximum bearing force (see figure 4.9) is almost 2 times higher than the maximum force in the linear analysis (see figure 3.8, resonance at about 12'650rpm), among others because the unbalance force is higher due to the higher speed.



- 18 -

### Shaft with REB

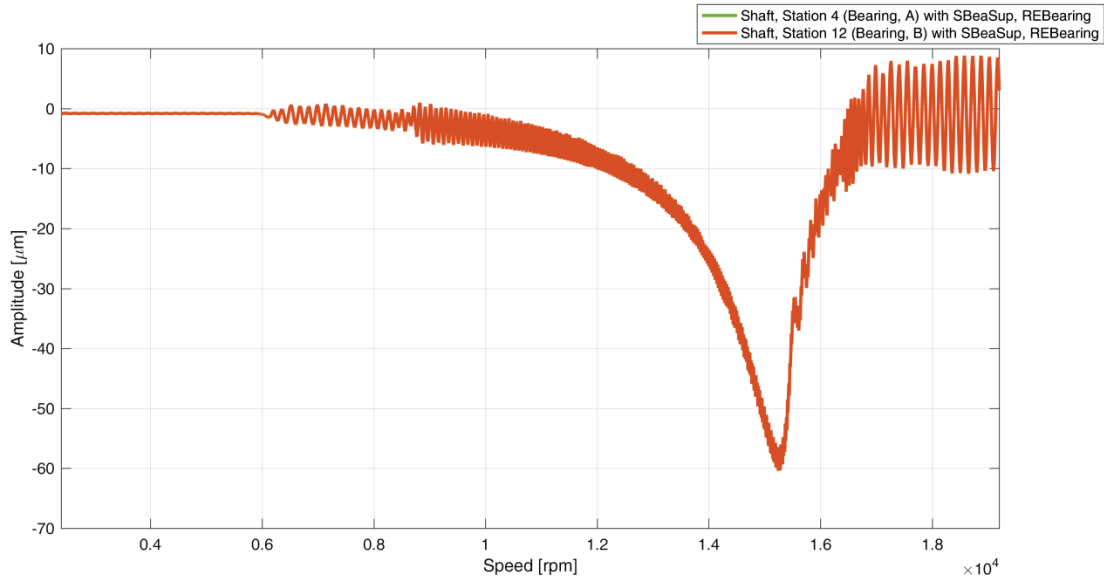
#### Transient Response Analysis

Load case: TransientNTCom 2 (Weight, Unbalance G2.5)

Analysis: 23-Nov-2016 16:42:44 - n(t), (without Prestress G2.5 (might be unstable)), init.cond. from SAN, nonlinear

Result Type: Axial displacement

Add. Modal Damping (all modes): 1 %



MADYN 2000 v.4.3.2

Fig. 4.8: Axial displacements at the bearings, run up from 20% to 160% in 5s, without axial preload

### Shaft with REB

#### Transient Response Analysis

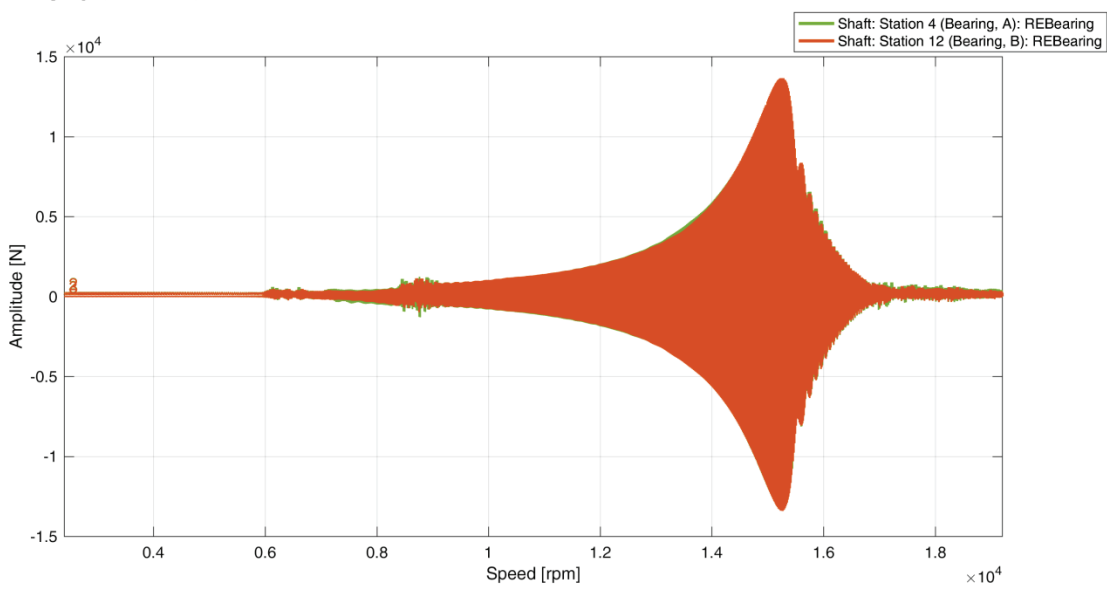
Load case: TransientNTCom 2 (Weight, Unbalance G2.5)

Analysis: 23-Nov-2016 16:42:44 - n(t), (without Prestress G2.5 (might be unstable)), init.cond. from SAN, nonlinear

Result Type: Bending forces

Add. Modal Damping (all modes): 1 %

Bold lines correspond to directions 2 and 2'



MADYN 2000 v.4.3.2

Fig. 4.9: Radial bearing forces, run up from 20% to 160% in 5s, without axial preload



- 19 -

### 4.3 Run Up without Axial Preload, Unbalance G1.0

The time histories of the radial displacements at the bearings for the run up of this case are shown in figure 4.10. A spectrum of the vibration of bearing A in 3- and 2-direction is shown in figure 4.11. The orbits at selected speeds at the bearings can be seen in figure 4.12. The time histories of the axial displacements at the bearings are shown in figure 4.13 and the radial bearing forces in figure 4.14.

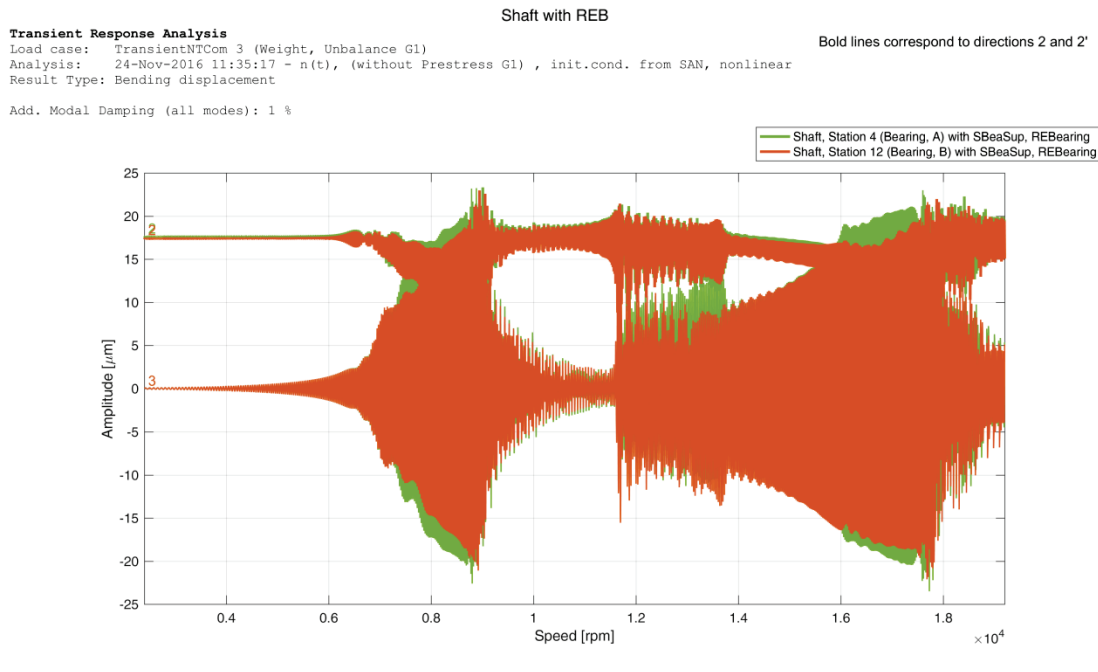


Fig. 4.10: Displ. at the bearings, run up from 20% to 160% in 5s, G1 Unb., without axial preload

In figure 4.10 no pronounced resonance can be recognized, especially for the 2-direction. The spectra in figure 4.11 with sub- and super-harmonic components indicate a heavy nonlinear behaviour. The orbits in figure 4.12 reveal that the rotor does not fully whirl within the clearance in the whole speed range. There is an increase of the vibration in the horizontal 3-direction until about 9'000rpm, which can be attributed to a horizontal resonance. At about 12'000rpm the vertical vibration suddenly increases together with the horizontal vibration, due to a vertical resonance (also see results of the linear analysis, figures 3.2 and 3.7). The horizontal vibration then further increases with increasing speed, but the dominant component then is a sub-harmonic at 50% speed as can be seen in the spectra of bearing A in figure 4.11. The orbit at 12'000rpm is that of a clear rocking motion. This sub-harmonic approaches a resonance at about 18'000rpm (50% of 18'000 corresponds to 9'000rpm, the resonance of the synchronous component).

The maximum vibration level is below 25 $\mu\text{m}$ , which is lower than the corresponding peak amplitudes in resonances for a linear analysis with this unbalance  $120\mu\text{m}/2.5 = 48\mu\text{m}$ . The 25 $\mu\text{m}$  have to be seen in relation to the clearance of 12 $\mu\text{m}$ , i.e. there is not much elastic deformation in the bearing.

The axial vibration remains low and for this case there is no pronounced shift at any speed as in the previous cases.

The maximum radial bearing forces in figure 4.14 are lower than the forces in the previous cases, approximately 1/3 compared to the case with preload and G2.5, which corresponds roughly to the ratio of the unbalances, but only 1/15 to the case without preload and G2.5.



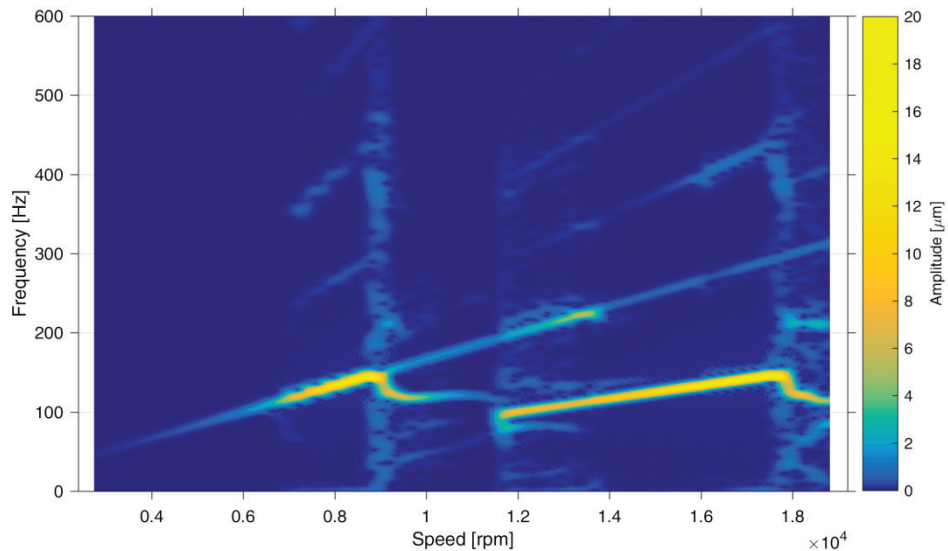
- 20 -

### Shaft with REB

**Transient Response Analysis - Spectrogram**  
 Load case: TransientNTCom 3 (Weight, Unbalance G1)  
 Analysis: 24-Nov-2016 11:35:17 - n(t), (without Prestress G1) , init.cond. from SAN, nonlinear  
 Result Type: Bending displacement

Add. Modal Damping (all modes): 1 %

Direction 3, Shaft, Station 4 (Bearing, A) with SBeaSup, REBearing



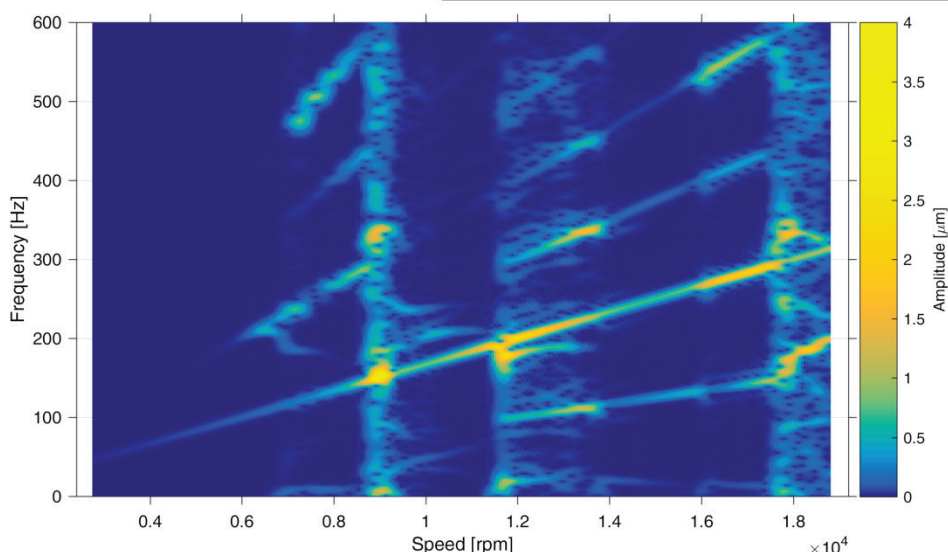
MADYN 2000 v.4.3.2

### Shaft with REB

**Transient Response Analysis - Spectrogram**  
 Load case: TransientNTCom 3 (Weight, Unbalance G1)  
 Analysis: 24-Nov-2016 11:35:17 - n(t), (without Prestress G1) , init.cond. from SAN, nonlinear  
 Result Type: Bending displacement

Add. Modal Damping (all modes): 1 %

Direction 2, Shaft, Station 4 (Bearing, A) with SBeaSup, REBearing



MADYN 2000 v.4.3.2

Fig. 4.11: Spectrum of the displacements at bearing A in 3- and 2-direction

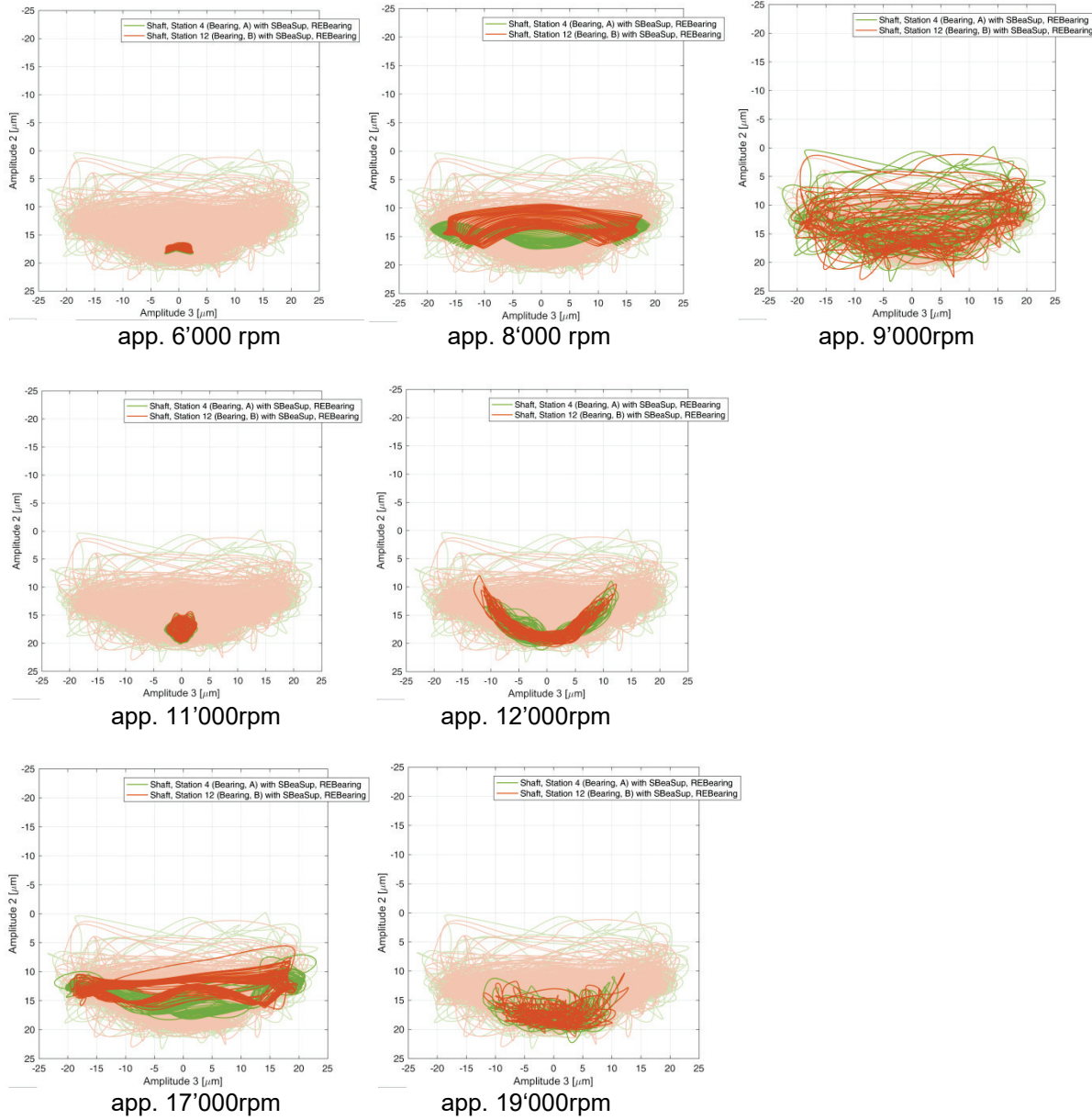


Fig. 4.12: Orbits at the bearings during run up, Unb. G1, without axial preload



- 22 -

### Shaft with REB

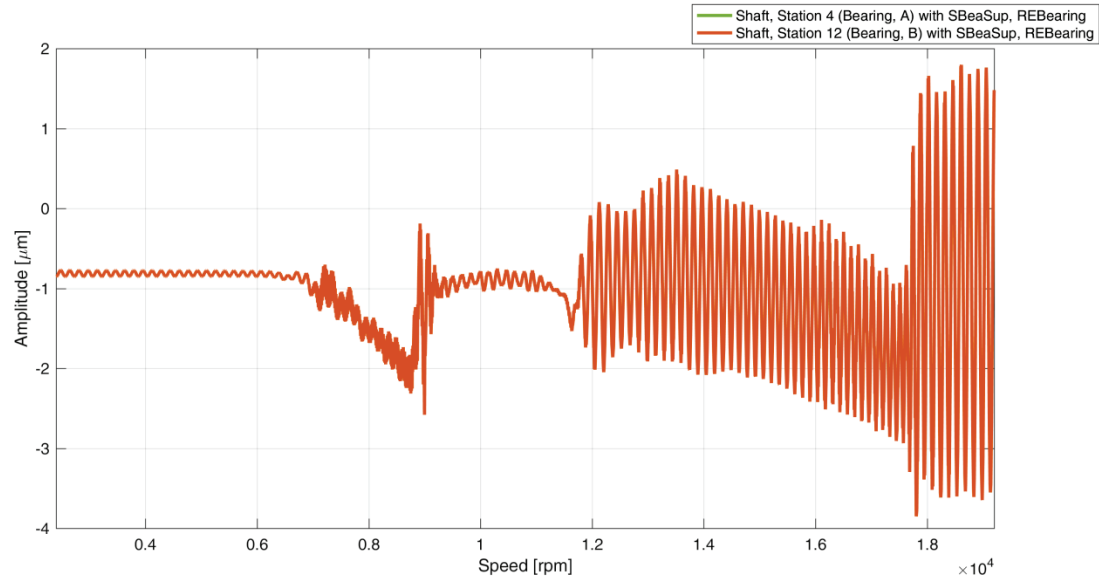
#### Transient Response Analysis

Load case: TransientNTCom 3 (Weight, Unbalance G1)

Analysis: 24-Nov-2016 11:35:17 - n(t), (without Prestress G1) , init.cond. from SAN, nonlinear

Result Type: Axial displacement

Add. Modal Damping (all modes): 1 %



MADYN 2000 v.4.3.2

Fig. 4.13: Axial displacements at the bearings, run up from 20% to 160% in 5s, G1 Unb., without axial preload

### Shaft with REB

#### Transient Response Analysis

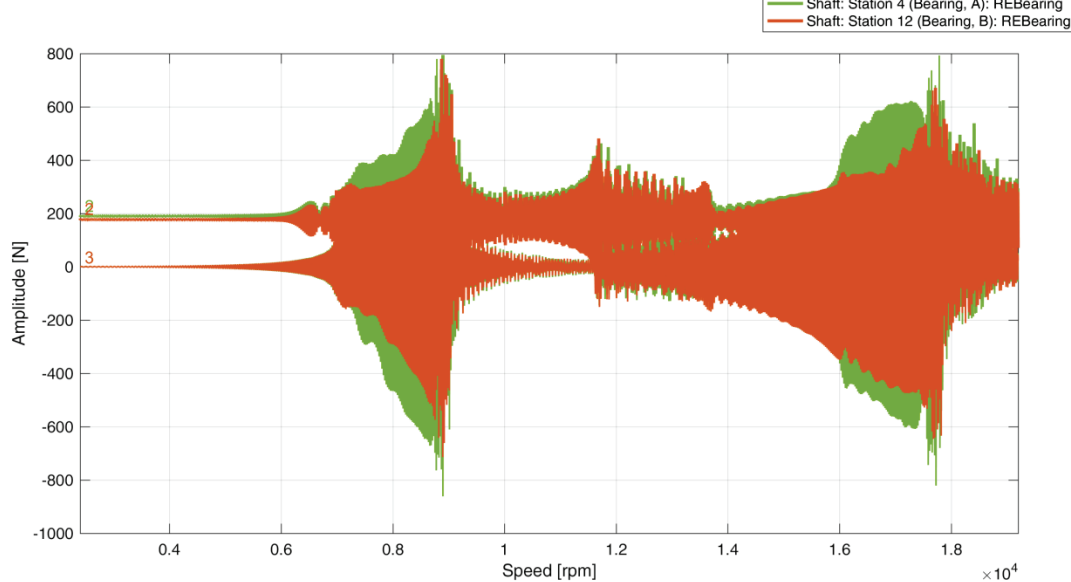
Load case: TransientNTCom 3 (Weight, Unbalance G1)

Analysis: 24-Nov-2016 11:35:17 - n(t), (without Prestress G1) , init.cond. from SAN, nonlinear

Result Type: Bending forces

Add. Modal Damping (all modes): 1 %

Bold lines correspond to directions 2 and 2'



MADYN 2000 v.4.3.2

Fig. 4.14: Radial bearing forces, run up from 20% to 160% in 5s, G1 Unb., without axial preload



## 5. Conclusions

Nonlinear transient analyses of a typical rotor supported on deep groove rolling element bearings can yield completely different results than a linear harmonic response analysis. The resulting behaviour can be complex and show various nonlinear effects such as sub-harmonics, super-harmonics as well as resonances of these non-synchronous components.

The run ups of three cases were analysed:

1. A case with axially preloaded bearings
2. A case with axially unloaded bearings
3. A case with axially unloaded bearing and low unbalance level

In case 1 with preloaded bearing the response is practically only synchronous and the amplitudes are quite similar to the linear analysis in a wide speed range. However, in resonance the behaviour is different. The speed with maximum vibration is below the linear resonance speed. The difference is caused by the nonlinear axial radial coupling at high radial loads. The high radial load forces the balls into a more centred position in the groove, causing an axial shift, new contact angles and a change of the bearing stiffness. The vibration in resonance is lower than in the linear case, which is to some extent due to the unsteady resonance condition.

In case 2 with axially unloaded bearings the behaviour of the nonlinear response is completely different from the linear behaviour. The lateral resonances in horizontal and vertical direction do not appear anymore. Instead a resonance at approximately the same speed as in case 1 appears. As in case 1 a nonlinear coupling with the axial direction occurs resulting in a considerable shift of the shaft in axial direction. The shift in this case is caused by the changed contact angle due to an increased bending when approaching the resonance. At certain speeds with low vibration level (low speeds and speeds above the resonance) sub-synchronous vibrations with a frequency of approximately 50% speed appear. They are caused by a kind of rocking motion of the shaft in the bearing with clearance. In a wide speed range below the resonance and in resonance the shaft fully whirls within the clearance. The vibrations below resonance are considerably higher than in the linear case due to the additional component of the clearance and the higher loading caused by this additional component. In the resonance the vibration is lower, than in the vertical resonance of the linear analysis, however the bearing forces are much higher.

In case 3 the behaviour is highly non-linear in the whole speed range. The shaft does not whirl within the clearance. The unbalance force is too low to lift the shaft to an upper contact. The vibrations have large sub-synchronous components and super-synchronous components. In vertical direction no clear resonance is visible. In horizontal direction resonance-like vibration increases can be observed, which are caused by a synchronous resonance and sub-synchronous resonance. The vibration level and the bearing forces are moderate. Axial vibrations remain very low and no axial shift as in the previous two cases occurs.